Automated Lung Nodule Candidate Detection Using An Iteratively Optimized Multi-Resolution 3D Depthwise Separable Cnns With Effective Training Initialization

V. Sumathi[1], Dr. V. Anuradha[2]

[1]*Research Scholar, Department of Computer Science, Sree Saraswathi Thyagaraja College, Pollachi, Tamil Nadu, India*
[2]*Head (PG), Department of Computer Science, Sree Saraswathi Thyagaraja College, Pollachi, Tamil Nadu, India*

ABSTRACT:
An earlier detection and diagnosis of lung cancer requires a major task known as lung nodule candidate classification. To detect the lung nodule candidate, a Multi-Resolution 3-Dimensional Convolutional Neural Network and Knowledge Transfer (MR3DCNN-KT) model has been designed that can extract the contextual information between multiple samples of lung nodule image for increasing the detection accuracy. But, this model was not able to classify few types of nodules that may cause the false detection. Also, the training data preparation was high difficult due to the manual labeling that consumes more time and the label mistakes were introduced while using large scale datasets since 3D-CNN requires more number of samples. Hence this article proposes an Iteratively Optimized MR3DCNN-KT (IO-MR3DCNN-KT) model that establishes automated weak label initialization to classify the large scale lung nodule image datasets. This model is trained on dynamically updated training datasets in an iterative manner. A Fast and Automatic Weak Labeling(FAWL) scheme is applied to generate the initial training dataset. Nonetheless, the computational complexity of 3D-CNN structure is extremely high since it requires the significant number of computational resources. As a result, an IO-MR3D Depthwise Separable CNN and KT (IO-MR3D-DSCNN-KT) model is proposed that introduces the bottleneck-based 3D-DSCNN structure to reduce the computational complexity. This model can extract both spatial and temporal features using basic depthwise convolution (conv)and pointwise conv, accordingly. Based on this model, the number of parameters used in the 3D-CNN structure is significantly reduced to automatically classify the lung nodule candidates. Finally, the experimental outcomes show that the IO-MR3D-DSCNN-KT model promises increased accuracy and robustness compared to the IO-MR3DCNN-KT and MR3DCNN-KT models.

Keywords— Bottleneck-based CNN, depthwise convolution, lung nodule candidate detection, MR3DCNN-KT, pointwise convolution, weak label initialization.

I. INTRODUCTION

Lung carcinoma is actually major causes of death and is stated to have poor levels of post-diagnosis survival in developing and undeveloped nations. Nevertheless, lung cancer may have a greater possibility of being recovered successfully if it is diagnosed immediately instead of later. The prognosis of this carcinoma is on the basis of pulmonary or lung nodule classification.An essential means of successful medical treatment and avoidance of lung cancer is early lung nodule classification. The key recommendation for the classification of lung nodules will also be the Computed Tomography (CT) scans [1]. In fact, spatial analysis of CT images is a long-term

method for radiological experts, since hundreds of samples are usually present on a specific scan and fewer than 100 voxels are available on a given nodule.

Modern Computer-Aided Detection (CAD) technologies have also beeninnovated to identify tiny nodules of the lung. This can be separated into CADe (Detection system) and CADs (Diagnostic system) [2-3]. CADe's primary objective is to identify Region-Of-Interests (ROIs) in the image, which may reveal different changes while the CADs's objective is to diagnose observed changes by category, volume, level and progress of epidemics. Two methods include the treatment of pulmonary nodules via CADs: raw nodule classification and nodule candidate detection [4].The detection is important to the specific choice of lung nodules. The detection of a nodule candidate does also pose many difficulties such as radiological fluctuation and may lead some nodules to be invisible, while other non-nodules are termed as lung nodules that vary in scales and structure. To avoid these limitations, an MRCNN-KT model was suggested in which standard 2D-CNN algorithm was enhanced as the new MR model via transferring its knowledge [5]. In this model, the knowledge was transferred from the source training processes and thus each side-output branch were taken for analyzing the features of different scales and resolutions from different depth layers in the CNN that classifies the lung nodule candidates. Moreover, objective and loss functions were developedas image-wise instead of pixel-wise representations. Further, samples creation and data augmentationwere achieved for both training and testing the adapted classifier for identifying pulmonary nodule candidates. Though the absolute lung nodule was often scattered on many samples, this 2D-CNN framework was restricted to extract the context features between multiple samples.

So, an MR3DCNN-KT model was introduced [6] to extract the context features between many samples. In this model, $3Dconv$ were utilized for extracting the spatial and temporal features so that the context features encoded in the many neighboring samples were discovered. Based on this model, many channels of data were created from the input frames and the data from all the channels was combined for defining the final feature vector. Moreover, the outputs of high-level features were regularized and variety of outputs from CNN models was fused for increasing the detection accuracy. On the contrary, few types of nodules were not completely defined or classified which may lead to the false detection of lung nodule candidates.Although 3D-CNN for lung nodule candidate classification has high accuracy with an acceptable error for incorrectlylabeled training networks, the training data preparation has high complexity since manual labeling was time-consuming and may introduce label errors in large scale datasets.Also, 3D-CNN needs more amount of samples than the 2D-CNN structure.

Therefore in this paper, an Iteratively Optimized MR3DCNN-KT (IO-MR3DCNN-KT) model is proposed that introduces automated weak label initialization for classifying the largescale datasets. This proposed IO-MR3DCNN-KT model is iteratively trained on dynamically updated training datasets. Particularly, the preliminary training dataset is created based on the FAWL scheme that utilizes the highest rate of spatial overlap method. On the other hand, the 3D-CNN algorithm has high computational complexity due to its significant amount of computational resources.Hence, an IO-MR3D Depthwise Separable CNN and KT (IO-MR3D-DSCNN-KT) model is proposed for reducing the computational complexity. In this model, a bottleneck-based 3D-DSCNN structure is introduced wherein the CT scan (lung nodule) image slices is split into spatial and temporal information. For learning spatial information, a fundamental depthwise$conv$notion is applied to each lung image whereas the 3D pointwise $conv$is applied for learning the temporal information i.e, the linear combination among sequential lung nodule image slices. This $conv$is modified for reducing the parameter sizes of the 3D-CNN and efficiently achieving the lung nodule candidate detection. Thus, this model can reduce the computational complexity of 3D-CNN structure and learn the large scale lung nodule image datasets with labbeling weak labels automatically.

II. Literature Survey

A multi-kernel based method [7] was proposed for selecting the features and learning the imbalanced data of pulmonary nodule. In this method, a multi-kernel feature choice was carried

out to learn the imbalanced data on the basis of pairwise similarities from the feature level and a multi-kernel over-sampling. However, it has high computational complexity.

A newlung nodule identification scheme [8] was proposed by means of Deep CNN (DCNN). Initially, a deconvolutionalframework was presented to Faster Region-based CNN (Faster R-CNN) for detecting lung nodule candidates on axial slices. After that, a 3D-DCNN was proposed with the aid of dropout scheme for reducing the false positive in candidate detection. However, the data between the small patches was not considered.

A novel approach was proposed using 3D-CNN [9] to minimize the False Positive (FP) in identifying the lung nodule automatically. In this approach, more affluent spatial features were encoded and more representative features were extracted by their hierarchical structure trained with 3D samples. Also, an effective method was applied to encode the multilevel context information. Then, the finalized outcomes were acquired via merging the likelihood outcomes of CNN. But, the variances between huge variants of lung nodules and the restricted training dataset were not resolved.

A novel multi-view multi-scale CNN [10] was proposed for classifying the types of lung nodules from CT images. Initially, the spherical surface centred at nodules was approximated by icosahedra and the normalized sampling was captured for CT scores on every spherical view at the highest radius. Then, intensity evaluation was performed by means of the sampled values for measuring each nodule's radius. After that, the re-sampling was built followed by the high-frequency data analysis for choosing which views were richer in information. At last, the nodule at ranked scales and views were constructed for pre-training the view independent CNNs and training the multi-view CNNs with the max-pooling. However, it cannot detect the tiny nodules and juxta-pleural nodules effectively.

A new Multi-scale Gradual Integration CNN (MGI-CNN) algorithm [11] was suggested to learn the feature representations of multi-scale inputs. In this algorithm, three major schemes were applied such as exploiting multi-scale inputs including various levels of context features, employing abstract information feature in various inputs scales with GI and training multi-stream feature fusion. Nonetheless, this algorithm has high FP rate.

A fusion algorithm [12] was introduced by fusing handcrafting features and the features trained at the 3D-CNN's output layers. Originally, various handcrafted features were extracted along with the intensity, geometric and texture features via the gray-level co-occurrence matrix. Afterwards, 3D-CNNs were trained for extracting the CNN features trained at the output layer. For every 3D-CNN, the CNN features integrated with the handcrafted features were given as the input to the SVM with the sequential forward feature choice algorithm to elect the best feature subset and built the classifiers. But, it has less robustness.

III. Proposed Methodology

Initially, an IO-MR3DCNN-KT model is described using automated weak label initialization scheme. Then, an IO-MR3DSCNN-KT model is explained.The block diagram of this proposed pulmonary nodule candidate identification models is portrayed in Figure 1.
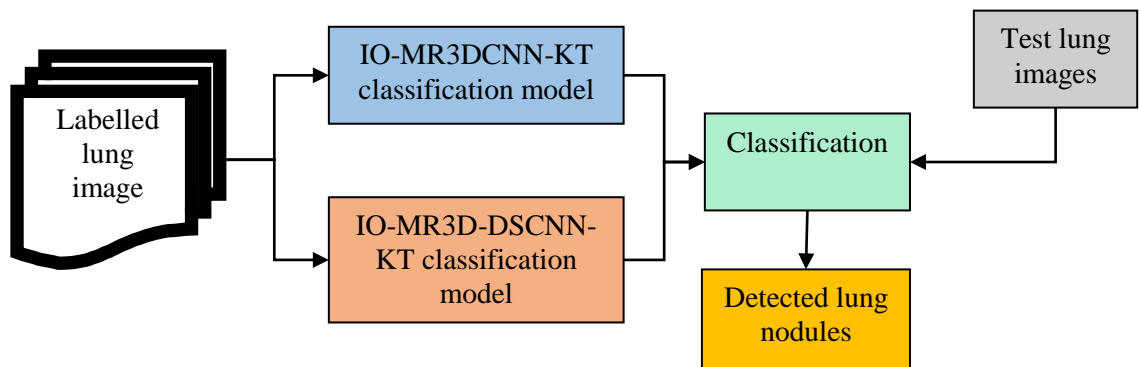
Figure 1. Block Diagram for Proposed Lung Nodule Detection Model

3.1 An Iterative Optimization Of MR3DCNN-KT With Automated Weak Label Initialization For Lung Nodule Candidate Detection

Initially, the lung images are acquired from the Kaggle's Data Science Bowl 2017 (KDSB17) dataset. This dataset provides CT scan images of patients including their cancer status. But, it does not offer the positions or sizes of lung nodules. It comprises 2101 axial scans of patient chest cavities. Of the 2101, 1261 are belonging to the training set and 840 are belonging to the testing set. Each CT scan is labeled as "with cancer" if the related patient is diagnosed with cancer within 1 year of the scan; or else, labeled as "without cancer".

Pre-processing

Every scan is comprised of manifold 2D axial scans taken in sequence with pixel values in the range $(-1024,3071)$ respective to Hounsfield radiodensity units. The amount of slices, their thickness and scales are varied between each scan. Also, noise removal, spatial smoothing, temporal pre-whitening and linear registration to the lung template space are performed by the FSL FLIRT and FEAT commands.Once pre-processing is completed, the dictionary learning and sparse coding methods are used for functional lung networks restoration for all patients. The dictionary learning input is a matrix $X \in \Re^{t \times n}$ with t rows and n columns having normalized image pixels from n lung voxels of a patient.

The outcome has a learned dictionary D and a sparse coefficient matrix $a \in \Re^{m \times n}$ with respect to $X = D \times a + \varepsilon$ where ε denotes the error and m denotes the fixed dictionary size. After that, a 3D spatial map of functional lung network is mapped with every row of the output coefficient matrix a.

IO-MR3DCNN-KT

This novel IO-MR3DCNN-KT is iteratively trained on dynamically updated training datasets. In particular, the preliminary training dataset is created by FAWL scheme that uses the maximal spatial overlap rate scheme for increasing the accuracy on detection with adequate training initialization. The classification labels are generated from KDSB17 dataset via clustering method according to the spatial overlap rate. Based on the classification labels, the KDSB17 dataset is used for detecting the lung nodule candidates.

According to the classification labels from KDSB17 dataset and the separate functional networks resulting from KDSB17 dataset, the preliminary network labels are instinctively and approximately allocated to every network by computing the spatial overlap rate similarity matrix. The spatial overlap rate is computed as:

$$Overlap\ rate = \sum_{k=1}^{|V|} \frac{min(V_k, W_k)}{V_k + W_k/2} \qquad (1)$$

In Eq. (1), V_k and W_k are the activation scores of voxel k in network volume maps V and W, accordingly. The empirical thresholding process is applied on the similarity matrix for ensuring the accurateness of the preliminary label assignment. For every separate network map, the label is allocated as classification labels whose spatial overlap rate is the highest amid each classification label. If not any similarity is higher than 0.2, then the label 0 is allocated to the respective network map and this label is not used for training.The IO-MR3DCNN-KT training can iterate over l input 3D network maps for the highest I iterations, initiating with the preliminary weak labels according to the spatial overlap rate. This spatial overlap rate-based classification achieves higher accuracy on detection while the CNN is able to correct the label for detection with increased accurateness.

This label alteration ability is adopted in this IO-MR3DCNN-KT model for increasing the previously allocated training labels in every iteration and so applying the alterations between labels after and before training. Once the iterative optimization is completed, a trade-off is ensured by IO-MR3DCNN-KT model while no significant changes happens; thus providing the optimized and efficiently trained MR3DCNN-KT for identifying the functional lung nodules.

Algorithm: IO-MR3DCNN-KT Training Process

Input: KDSB17 dataset

1. Compute pairwise overlap rate between separate functional networks and functional labels $\rightarrow l \times n$ similarity matrix S^0;
2. Set threshold overlap rate value in S less than 0.2 to be 0;

$\qquad \boldsymbol{for}\big(\text{each individual network row } S_i^0 \text{ in } S^0\big)$

$\qquad\qquad \boldsymbol{if}\big(S_i^0 = 0\big)$

$\qquad\qquad\qquad label_i = 0;$

$\qquad\qquad \boldsymbol{else}$

$\qquad\qquad\qquad label_i = argmax\big(S_i^0\big);$

$\qquad\qquad\qquad \{argmax\big(S_i^0\big) \in N | 1 \leq argmax\big(S_i^0\big) \leq n\};$

$\qquad\qquad \boldsymbol{end\ if}$

$\qquad \boldsymbol{end\ for}$

$\qquad$ **Return** $label^0$

//MR3DCNN-KT Training: using non-zero labeledseparate functional networks and $label^0$ as preliminary training sets

$\qquad \boldsymbol{for}(i \in \{0,1,2,\dots,maxIter\})$

$\qquad\qquad$ Train MR3DCNN-KT on

$\qquad\qquad\qquad \big[no\ zero\ labeled\ individual\ functional\ networks, label^i\big]$

$\qquad\qquad label^{i+1} = MR3DCNN - KT_{model}\text{classify on all functional networks};$

$\qquad\qquad label\_var = var\big(label^i, label^{i+1}\big)$

$\qquad\qquad \boldsymbol{if}(|label_{var}|/l < 0.4\%)$

$\qquad\qquad\qquad$ **Break**

$\qquad\qquad \boldsymbol{end\ if}$

$\qquad \boldsymbol{end\ for}$

$\qquad$ **Return**$MR3DCNN - KT_{model}$

Though it achieves better accuracy on detection of lung nodules, this 3D-CNN has high computational complexity due to the requirement of amount of parameters in 3D-CNN model. The 3D-CNN parameter is computed as:

$$P_{3D} = n \times c \times d(k \times k + 1) \qquad (2)$$

In Eq. (2), n denotes the amount of filters, k represents the spatial size of the $conv$kernel, d denotes the amount of temporal images and c indicates the amount of channels. When the input channels increase, the amount of parameter also increases. To tackle this problem, IO-MR3D-DSCNN-KT model is proposed which is explained below.

3.2 Effective Lung Nodule Candidate Detection Using Iteratively Optimized Multi-Resolution 3D-Depthwise Separable CNN And Knowledge Transfer

A novel IO-MR3D-DSCNN-KT model is proposed for effectively understanding the haptic force from lung images. For this purpose, the image is split as spatial and temporal details which are trainedindividually and consecutively. The processes performed in this model are:

1. Spatial feature extraction: The 2D depthwise$conv$ is performed on every slice of the input image i.e., the task of training the spatial data free of the channel is performed on every slice.
2. Temporal feature extraction: The 3D pointwise$conv$ is used for learning the linear mixture of channels among the channels of neighborslices.

Initially, the spatial data is extracted by this 3D-DSCNN structure that applies the 2D depthwise$conv$filters in the images. In this model, the shared weight parameters are used and the amount of these parameters is significantly reduced compared to the standard 3D-CNN model. Similarly, the 3D pointwise $conv$filters are applied for extracting the temporal feature extraction. The concept of proposed IO-MR3D-DSCNN-KT model is shown in Figure 2.

The depthwise$conv$filters $F_{depthwise} \in \Re^{k \times k}$ are trained separately based on their respective channels. This filter is fused with the pointwise $conv$filter $F_{pointwise} \in \Re^{1 \times 1}$ for training the relationshipbetween the channels in each layer. While increasing the input channels, only the respective amount of filters is increased whereas the amount of parameters used in the standard

3D-CNN model is not increased. Therefore, the dimensions of the weight parameters are also calculated as:

$$P_{3D} = n \times (c \times d + 1) + c \times (k \times k + 1) \qquad (3)$$
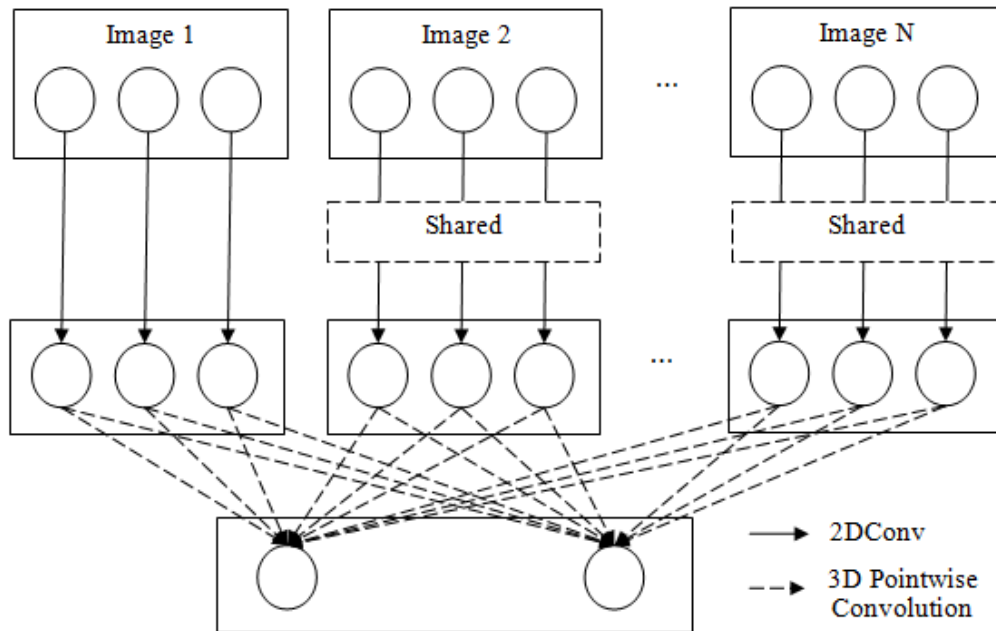
Figure 2. Concept of Proposed IO-MR3D-DSCNN-KT Model
This bottleneck 3D module is illustrated in Figure 3for the inverted residual and fundamental linear block-based units. The primary layer of this unit to enlarge the amount of channels is the pointwise $conv$. The secondary layer is the depthwise$conv$filter with a $a \times a$ kernel and the 3D pointwise $conv$is applied in the last layer to train the temporal data. Also, the depthwise$conv$filters are stacked perfectly for converting the temporal data to the salient data for detecting the lung nodules.The specifications of the IO-MR3D-DSCNN-KT network structure are given in Table 1.

Table 1. Details of Network Structure of the IO-MR3D-DSCNN-KT Model

Layers	Expand Channels	Output Channels	Spatial Stride	Kernel Depth	Depth Stride
Conv2D 3 × 3	-	32	1	1	1
Bottleneck 3D 3 × 3 (a)	32	16	1	1	1
Bottleneck 3D 3 × 3 (a)	64	24	1	1	1
Bottleneck 3D 3 × 3 (a)	96	32	1	1	1
Bottleneck 3D 3 × 3 (b)	128	64	2	3	2
Bottleneck 3D 3 × 3 (b)	192	92	2	3	2
Bottleneck 3D 3 × 3 (b)	384	128	2	3	2
Bottleneck 3D 3 × 3 (b)	448	192	2	3	2
Conv2D 1 × 1	-	1280	2	2	2
Avg. Pool. *4 × 4*	-	-	1	1	-
Fully Connected (FC) 1	-	1	-	-	-

(a)   (b)
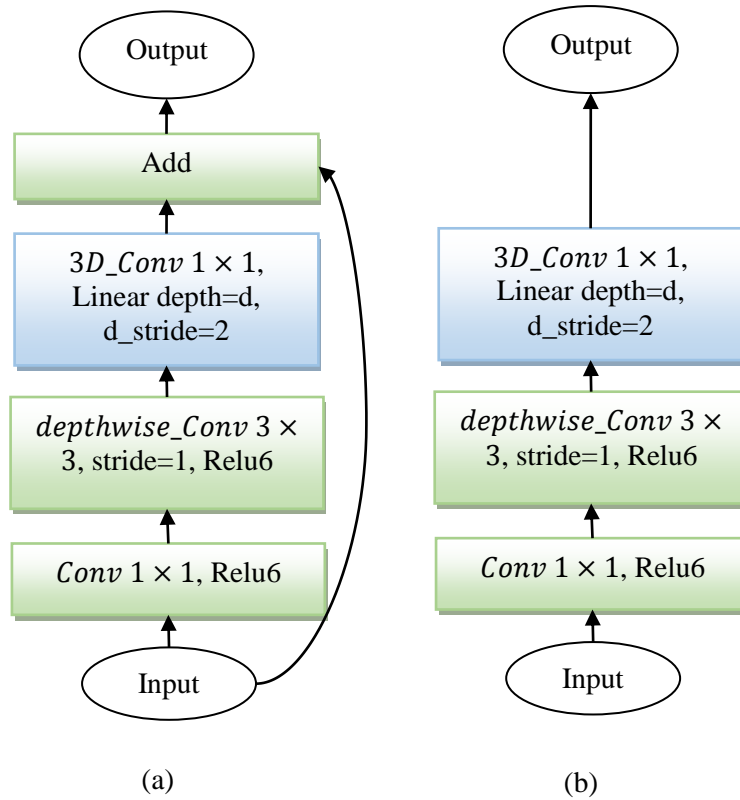
Figure 3. IO-MR3D-DSCNN-KT Model on the basis of (a) Inverted Residual Block and (b) Linear Block (Depthwise*conv*Filter)

IV. EXPERIMENTAL RESULTS

The performance of IO-MR3DCNN-KT and IO-MR3D-DSCNN-KT models is evaluated as well as compared with the MR3DCNN-KT model using MATLAB 2018a. Given a KDSB17 dataset, 1261 data are used for training and 840 data are used for testing process. This comparative analysis is performed based on different metrics such as precision, recall, f-measure, accuracy, error rate and separability. Figure 4 portrays the results of detected nodules usingIO-MR3DCNN-KT and existing MR3DCNN-KT models. Similarly, Figure 5 illustrates the outcomes of detected nodules using IO-MR3D-DSCNN-KT and IO-MR3DCNN-KT models.
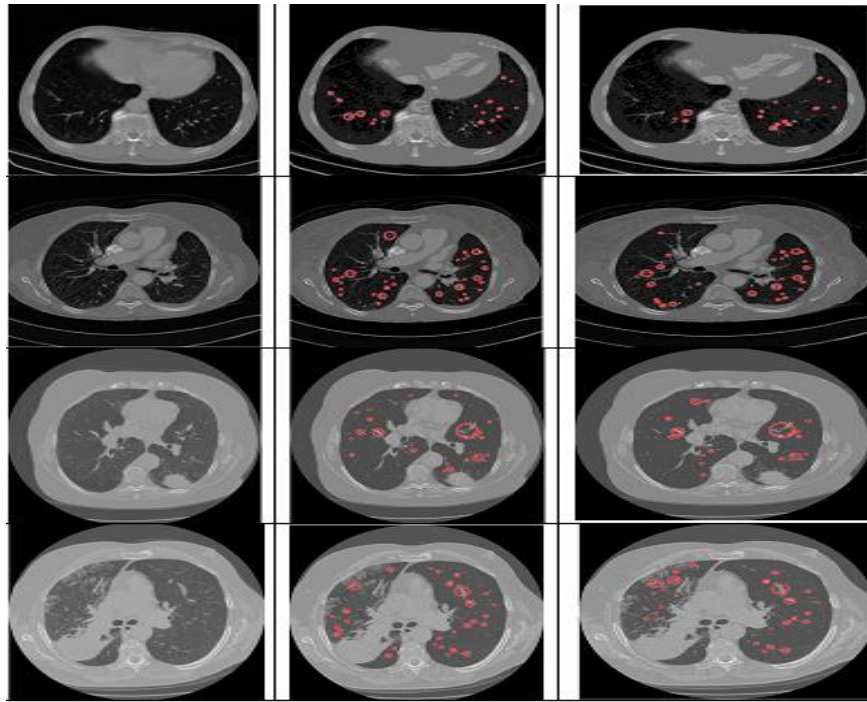
(a)   (b)   (c)

Figure 4. Results of Lung Nodule CandidateDetection Models: (a) Input Image (b) Detected Nodules using MR3DCNN–KT (c) Detected Nodules using IO-MR3DCNN–KT
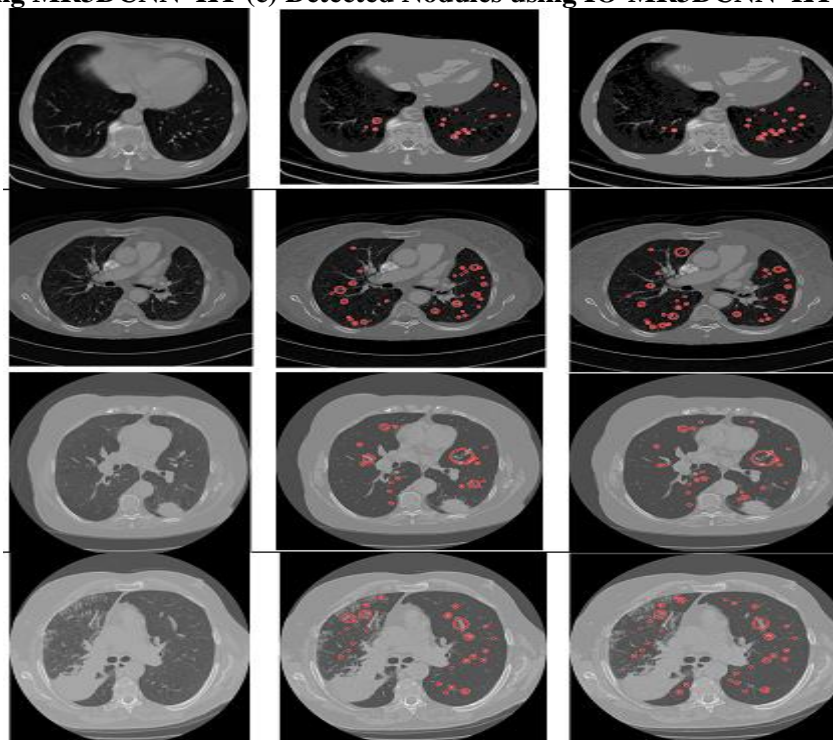
(a)   (b)   (c)

Figure 5. Results of Lung Nodule Candidate Detection Models: (a) Input Image (b) Detected Nodules using IO-MR3DCNN–KT (c) Detected Nodules using IO-MR3D-DSCNN–KT

4.1 PRECISION

It is a measure computed based on the detection of lung nodules at True Positive (TP) and False Positive (FP) rates.

$$Precision = \frac{TP}{TP+FP} \qquad (4)$$
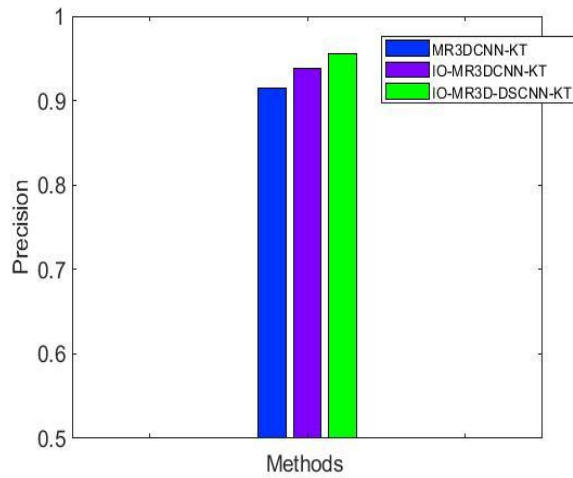
Figure 6. Comparison of Precision

In Figure 6, the precision values for IO-MR3D-DSCNN-KT, IO-MR3DCNN-KT and MR3DCNN-KT models are illustrated. Through this analysis, it is recognized that the precision of IO-MR3D-DSCNN-KT is 1.84% higher than the IO-MR3DCNN-KT and 4.52% higher than MR3DCNN-KT models.

4.2 Recall

It is calculated on the basis of detecting the lung nodules at TP and False Negative (FN) rates.

$$Recall = \frac{TP}{TP+FN} \qquad (5)$$
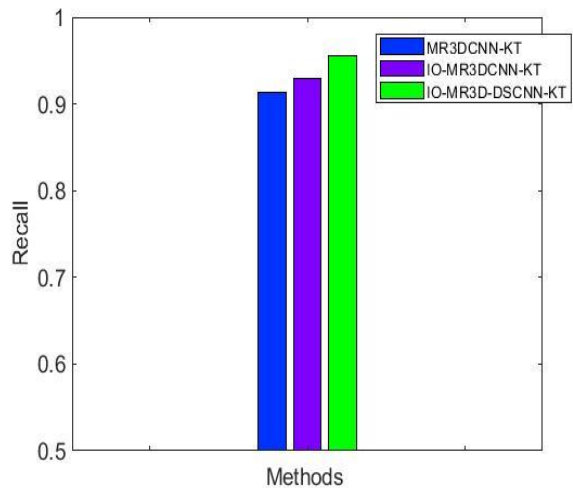
Figure 7. Comparison of Recall

Figure 7 shows the recall values for IO-MR3D-DSCNN-KT, IO-MR3DCNN-KT and MR3DCNN-KT models. By using this analysis, it is noticed that the recall of IO-MR3D-DSCNN-KT is 2.68% higher than the IO-MR3DCNN-KT and 4.53% higher than MR3DCNN-KT models.

4.3 F-Measure

It is the harmonic mean of both precision and recall.

$$F - measure = \frac{2 \cdot Precision \cdot Recall}{Precision + Recall} \qquad (6)$$
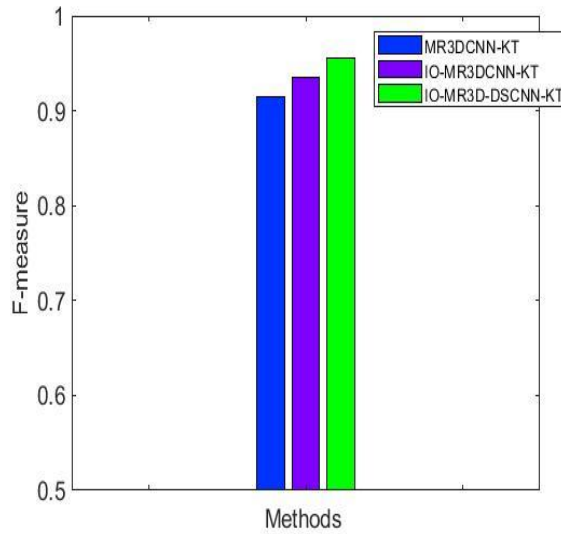
Figure 8. Comparison of F-measure
In Figure 8, the f-measure values for IO-MR3D-DSCNN-KT, IO-MR3DCNN-KT and MR3DCNN-KT models are illustrated. From this analysis, it is observed that the f-measure of IO-MR3D-DSCNN-KT is 2.18% higher than the IO-MR3DCNN-KT and 4.53% higher than MR3DCNN-KT models.

4.4 Accuracy
It is the ratio of accurate lung nodule detection over the total amount of instances evaluated.

$$Accuracy = \frac{TP + True\ Negative\ (TN)}{TP + TN + FP + FN} \qquad (7)$$
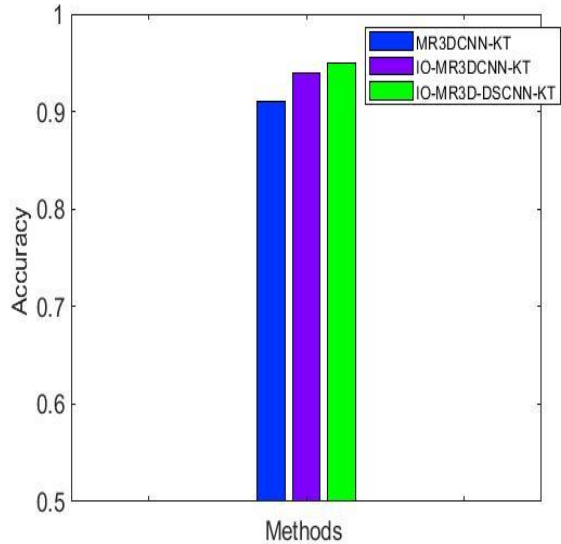
Figure 9. Comparison of Accuracy
Figure 9 shows the accuracy values for IO-MR3D-DSCNN-KT, IO-MR3DCNN-KT and MR3DCNN-KT models. From this analysis, it is addressed that the accuracy of IO-MR3D-DSCNN-KT is 1.06% higher than the IO-MR3DCNN-KT and 4.4% higher than MR3DCNN-KT models.

4.5 Error Rate

It is measured as:

$$Error\ rate = \frac{FP+FN}{TP+TN+FP+FN} \qquad (8)$$
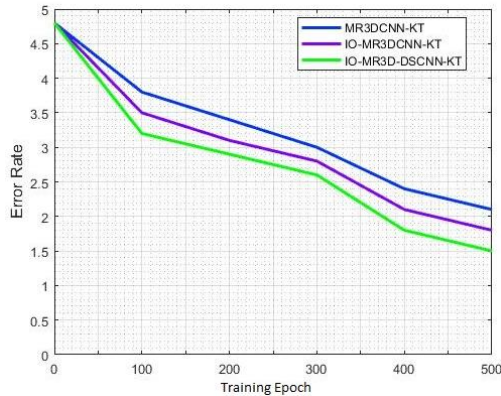
Figure 10. Comparison of Error Rate

In Figure 10, the error rate values for IO-MR3D-DSCNN-KT, IO-MR3DCNN-KT and MR3DCNN-KT models are shown. From this analysis, it is observed that the error rate of IO-MR3D-DSCNN-KT is 27.12% less than the IO-MR3DCNN-KT and 28.57% less than MR3DCNN-KT models while considering 500 training epochs.

4.6 Separability

It is the separability of the data representation in different layers and computed as follows:

$$Separability = \frac{\sum_i (\overline{x^i} - \bar{x})^2}{\sum_i \frac{1}{n^i - 1} \sum_j (x_j^i - \overline{x^i})^2} \qquad (9)$$
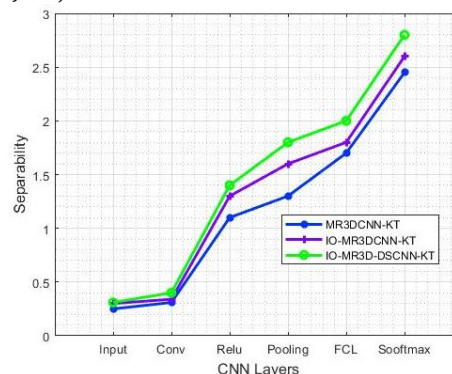
Figure 11. Comparison of Separability

Figure 11 shows the separability values of IO-MR3D-DSCNN-KT, IO-MR3DCNN-KT and MR3DCNN-KT models for different layers in CNN architecture. In case of softmaxlayer, the separability of IO-MR3D-DSCNN-KT is 7.69% higher than IO-MR3DCNN-KT and 14.29% higher than MR3DCNN-KT models.

V. CONCLUSION

In this article, an IO-MR3DCNN-KT model is proposed for achieving training initialization using automated weak labeling process. This model is mainly applied for generating the initial training dataset which is trained in an iterative manner. Thus, an IO-MR3D-DSCNN-KT model is proposed that comprises the bottleneck-based 3D-DSCNN architecture for minimizing the computational complexity of 3D-CNN structure. In this model, both spatial and temporal features are extracted via fundamental depthwise$conv$ and pointwise$conv$, correspondingly, for classifying the lung nodule candidates with reduced amount of parameters in the 3D-CNN structure. Finally, the experimental results proved that the IO-MR3D-DSCNN-KT model achieves better performance than the both IO-MR3DCNN-KT and MR3DCNN-KT models.

REFERENCES

[1] Bach, P. B., Mirkin, J. N., Oliver, T. K., Azzoli, C. G., Berry, D. A., Brawley, O. W., ... &Sabichi, A. L. (2012). Benefits and harms of CT screening for lung cancer: a systematic review. *Jama*, *307*(22), 2418-2429.

[2] Messay, T., Hardie, R. C., & Rogers, S. K. (2010). A new computationally efficient CAD system for pulmonary nodule detection in CT imagery. *Medical image analysis*, *14*(3), 390-406.

[3] Javaid, M., Javid, M., Rehman, M. Z. U., & Shah, S. I. A. (2016). A novel approach to CAD system for the detection of lung nodules in CT images. *Computer methods and programs in biomedicine*, *135*, 125-139.

[4] Setio, A. A. A., Traverso, A., De Bel, T., Berens, M. S., van den Bogaard, C., Cerello, P., ... & van der Gugten, R. (2017). Validation, comparison, and combination of algorithms for automatic detection of pulmonary nodules in computed tomography images: the LUNA16 challenge. *Medical image analysis*, *42*, 1-13.

[5] Zuo, W., Zhou, F., Li, Z., & Wang, L. (2019). Multi-resolution CNN and knowledge transfer for candidate classification in lung nodule detection. *IEEE Access*, *7*, 32510-32521.

[6] Arena, P., Basile, A., Bucolo, M., & Fortuna, L. (2003). Image processing for medical diagnosis using CNN. *Nuclear Instruments and Methods in Physics Research Section A: Accelerators, Spectrometers, Detectors and Associated Equipment*, *497*(1), 174-178.

[7] Cao, P., Liu, X., Yang, J., Zhao, D., Li, W., Huang, M., &Zaiane, O. (2017). A multi-kernel based framework for heterogeneous feature selection and over-sampling for computer-aided detection of pulmonary nodules. *Pattern Recognition*, *64*, 327-346.

[8] Ding, J., Li, A., Hu, Z., & Wang, L. (2017). Accurate pulmonary nodule detection in computed tomography images using deep convolutional neural networks. *arXiv preprint arXiv:1706.04303*, 1-9.

[9] Dou, Q., Chen, H., Yu, L., Qin, J., &Heng, P. A. (2017). Multilevel contextual 3-D CNNs for false positive reduction in pulmonary nodule detection. *IEEE Transactions on Biomedical Engineering*, *64*(7), 1558-1567.

[10] Liu, X., Hou, F., Qin, H., &Hao, A. (2017). Multi-view multi-scale CNNs for lung nodule type classification from CT images. *Pattern Recognition*, *77*, 262-275.

[11] Kim, B. C., Yoon, J. S., Choi, J. S., & Suk, H. I. (2019). Multi-scale gradual integration CNN for false positive reduction in pulmonary nodule detection. *Neural Networks*, *115*, 1-10.

[12] Li, S., Xu, P., Li, B., Chen, L., Zhou, Z., Hao, H., ...& Jiang, S. (2019). Predicting lung nodule malignancies by combining deep convolutional neural network and handcrafted features. *Physics in Medicine & Biology*, *64*(17), 1750